This is the accepted manuscript made available via CHORUS. The article has been published as:

Spinons and damped phonons in the spin-math xmlns="http://www.w3.org/1998/Math/MathML">mfrac>mn>1/mn>mn>2/mn>/mfrac>/math> quantum liquid math xmlns="http://www.w3.org/1998/Math/MathML">msub>mi mathvariant="normal">Ba/mi>mn>4/mn>/msub>msub> mi mathvariant="normal">Ir/mi>mn>3/mn> /msub>msub>mi mathvariant="normal">O/mi> mn>10/mn>/msub>/math> observed by Raman scattering

Aaron Sokolik, Sami Hakani, Susmita Roy, Nicholas Pellatz, Hengdi Zhao, Gang Cao, Itamar Kimchi, and Dmitry Reznik

Phys. Rev. B **106**, 075108 — Published 3 August 2022

DOI: 10.1103/PhysRevB.106.075108

Spinons and damped phonons in spin-1/2 quantum-liquid $Ba_4Ir_3O_{10}$ observed by Raman scattering.

Aaron Sokolik,[1] Sami Hakani,[2] Susmita Roy,[1] Nicholas Pellatz,[1]
Hengdi Zhao,[1] Gang Cao,[1] Itamar Kimchi,[2] and Dmitry Reznik[1]

[1] *Department of Physics, University of Colorado Boulder, Boulder, CO 80309*
[2] *School of Physics, Georgia Institute of Technology, Atlanta, GA 30332*

(Dated: October 28, 2021)

In spin-1/2 Mott insulators, non-magnetic quantum liquid phases are often argued to arise when the system shows no magnetic ordering, but identifying positive signatures of these phases or related spinon quasiparticles can be elusive. Here we use Raman scattering to provide three signatures for spinons in a possible spin-orbit quantum liquid material $Ba_4Ir_3O_{10}$: (1) A broad hump, which we show can arise from Luttinger Liquid spinons in Raman with parallel photon polarizations normal to 1D chains; (2) Strong phonon damping from phonon-spin coupling via the spin-orbit interaction; and (3) the absence of (1) and (2) in the magnetically ordered phase that is produced when 2% of Ba is substituted by Sr ($(Ba_{0.98}Sr_{0.02})_4Ir_3O_{10}$). The phonon damping via itinerant spinons seen in this quantum-liquid insulator suggests a new mechanism for enhancing thermoelectricity in strongly correlated conductors, through a neutral quantum liquid that need not affect electronic transport.

I. INTRODUCTION

Spin-1/2 magnetic insulators can avoid the conventional fate of magnetic order, by instead forming one of various types of exotic quantum liquid states. Such quantum liquids in 2D spin systems come in variously many flavors: gapped spin liquids such as the toric code [1–5], gapless spin liquids such as a spinon Fermi surface [3–5], sliding Luttinger liquids [6], and yet other examples whether recently discovered or yet to be discovered [3–5, 7]. Their common features include a high degree of quantum entanglement, and (typically) exotic "spinon"-type excitation. But beyond mere lack-of-ordering, positive signatures that identify a particular material as a quantum liquid state are difficult to access. Theoretical treatments of the strongly spin-orbit coupled honeycomb iridates and, more recently, α-$RuCl_3$ have inspired a large body of experimental work that anticipates a spin liquid [2, 8–15]. However, there has been no clear-cut material realization of a quantum spin liquid thus far, suggesting that a different material approach may also be fruitful.

Here we report on our observation and analysis of signatures of fractionalized spinons, through low temperature Raman spectroscopy of a recently discovered [16] quasi-2D spin-1/2 material, $Ba_4Ir_3O_{10}$. $Ba_4Ir_3O_{10}$ adopts a monoclinic structure with a $P2_1/c$ space group, which consists of Ir_3O_{12} trimers (with $Ir4^+(5d^5)$ ions) of face-sharing IrO_6 octahedra that are vertex-linked to other trimers, forming 2D sheets of a distorted square lattice in the *bc* plane, that are stacked along the a-axis with weak connectivity between the sheets (Fig. 1a). Electrical resistivity shows a clear insulating state across the entire temperature range measured up to 400 K. The strong spin-orbit-coupling and frustration of the Ir spin-1/2 moments conspire to form an unusual kind of highly frustrated quantum liquid state: $Ba_4Ir_3O_{10}$ shows no magnetic order down to 0.2 K, despite strong antiferromagnetic interactions with Curie-Weiss temperatures ranging from 100 K to 700 K [16]. This quantum liquid state shows a sizable linear heat capacity with a constant offset at very low temperatures, $C \sim T + C_0$ implying that the absence of magnetic ordering is accompanied by gapless quantum-fluctuating excitations. Linear (and surprisingly small) thermal conductivity is also observed at low temperatures, again consistent with the quantum liquid state. Finally, this quantum liquid state is evidently quite fragile and disappears upon slight perturbations to the crystal: experimentally, a mere 2% Sr substitution for Ba ($(Ba_{0.98}Sr_{0.02})_4Ir_3O_{10}$) precipitates conventional AFM order below 130 K, thereby eliminating the linear-T heat capacity and drastically changing magnetization and thermal conductivity.

Raman spectroscopy of the pure compound shows two unusual features at low temperature (Fig. 1b). First, phonon peaks are extremely broad corresponding to short lifetimes. Second, a broad hump centered near 180 cm^{-1} is present underneath the phonons. The hump persists across the range of all measured temperatures, 10 K to 170 K. Interestingly, slight Sr substitution for Ba, which induces antiferromagnetic order below 130 K, makes the phonons narrow and eliminates the broad hump (Fig. 1c). This suggests that the hump and the reduced phonon lifetimes are associated with the spin-1/2 excitation sector. At higher temperatures above the $(Ba_{0.98}Sr_{0.02})_4Ir_3O_{10}$ magnetic transition T_N, the broad hump is restored (Fig. 2).

Raman spectra presented here were obtained with a 671 nm solid state laser. All experiments were performed on a McPherson custom triple spectrometer equipped with a LN_2 cooled charge-coupled device (CCD) detector. It was configured in a subtractive mode with 1200 grooves per mm gratings in the filter stage and 1800 g/mm in the spectrometer stage. The sample was mounted in a

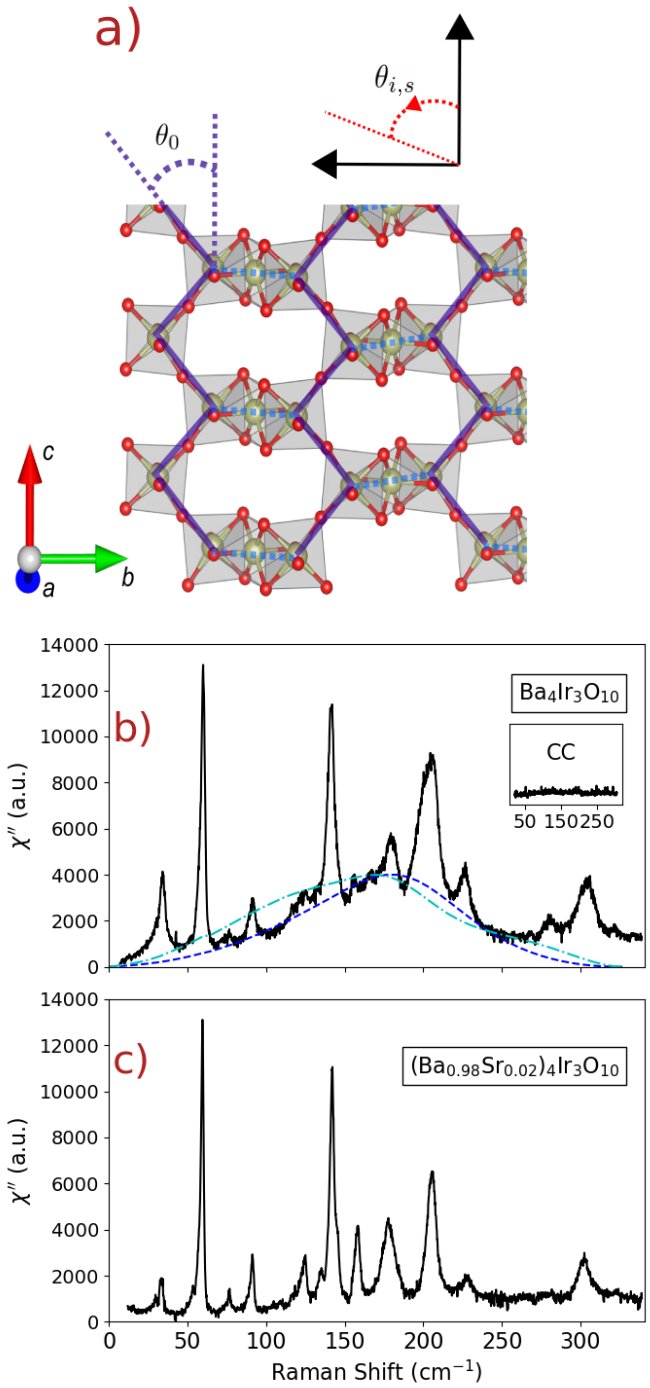

FIG. 1. Raman spectra of quantum liquid $Ba_4Ir_3O_{10}$, and the Sr-doped magnetically ordered sister compound ($(Ba_{0.98}Sr_{0.02})_4Ir_3O_{10}$). (a) $Ba_4Ir_3O_{10}$ is a 2D layered spin-1/2 magnet, featuring 1D zigzag chains coupled via trimers. $Ba_4Ir_3O_{10}$ is a 2D layered spin-1/2 magnet, featuring 1D zigzag chains coupled via trimers as originally shown in [16]. Note the angle theta and the coordinator are added to the figure for the convenience of discussion. (b,c) show Raman scattering spectra in *bb* photon polarization. The pristine compound features broadened phonon peaks on top of a broad hump, which is captured well by a four-spinon continuum in quantum liquid mean field theories with $J_{\rm eff}/k_B = 75$ K (R_1 dashed, blue; R_2 dot-dashed, cyan). Non-magnetic Sr substitution in $(Ba_{0.98}Sr_{0.02})_4Ir_3O_{10}$ produces non-frustrated magnetic order and eliminates the phonon broadening and the 4-spinon hump.

top-loading closed-cycle refrigerator. Phonons were observed only in the spectra measured with incident and scattered photon polarization parallel to the crystallographic b-axis (*bb* geometry) (Fig. 1a).

II. BROAD HUMP

We begin by discussing the broad hump feature in the Raman signal. As evident from Fig. 1b,c and Fig. 2, the spectral weight of the hump, as a function of Sr-substitution and temperature, is anticorrelated with the magnetic order parameter. This correlation already strongly implies that it is associated with excitations of the non-ordered quantum liquid of spins. Indeed it is reminiscent of the broad feature reported in the Raman spectra of the 1D magnet $CuGeO_3$, which is characterized by 1D spin chains with spinon excitations [17–23]. A multi-magnon mechanism for the hump is ruled out by the absence of magnetic ordering where the hump is present. Moreover a two-magnon continuum of free magnons at zero field (particle-hole symmetry) would host a Van Hove singularity of magnon joint density of states, as has been recently observed [24], but in contrast to the featureless hump seen here. The observed hump necessarily arises from a fractionalized excitation, which we will refer to as a spinon, and thus represents a four-spinon continuum.

III. THEORETICAL MODEL VIA SPINONS OF J_1-J_2-ZIGZAG CHAINS

To test this hypothesis, we construct a concrete theoretical model and use it to compute the expected Raman spectra of a four-spinon continuum. The theoretical model we use entails decoupled 1D zigzag chains. Even though $Ba_4Ir_3O_{10}$ is a quasi-2D magnet and clearly not a collection of 1D chains (neither microscopically nor phenomenologically; e.g., in its lack of Bonner-Fisher peak in susceptibility), it has been argued to be fruitfully modeled in terms of coupled 1D Heisenberg chains [16], providing a tractable theoretical model for spinons. Since these spinons are 1D spinons, and not necessarily the true 2D quantum liquid spinons, we expect the resulting model to approximately capture low energy physics but fail at higher energies or temperatures. Raman signals from decoupled 1D Tomonaga-Luttinger liquids have been computed in bosonization [22], which captures only the low-energy power-law onset of the four-spinon hump; numerically in small systems [25]; and in certain types of spinon mean field theories [18, 26, 27].

Here we compute the four-spinon Raman response in mean field, following Ref. [18] but also compute the mean field for an alternative equally-correct treatment, which has not been done before, and additionally point out an

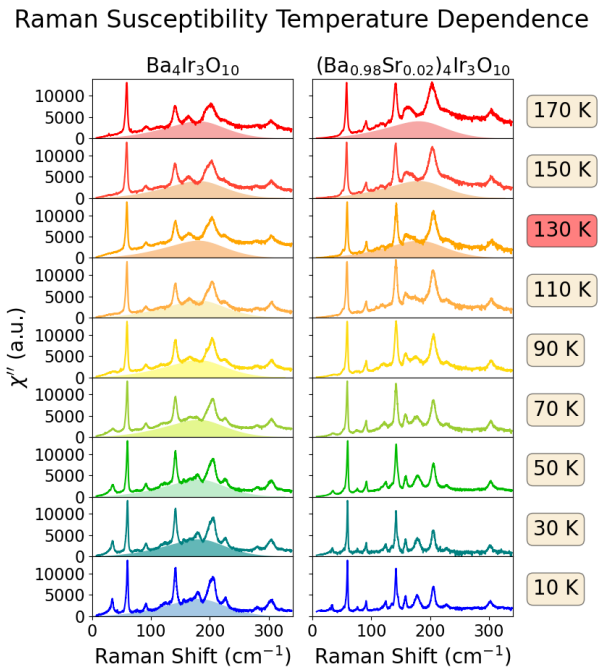

FIG. 2. Temperature dependence of Raman spectra in the *bb* photon polarization for both compounds. The $Ba_4Ir_3O_{10}$ broadened phonons and broad 4-spinon hump at 10 K (shaded) persist up to 170 K, but are absent in the magnetically-ordered sister compound ($(Ba_{0.98}Sr_{0.02})_4Ir_3O_{10}$) at all temperatures below its Néel temperature of 130 K.

important restriction related to the *bb* parallel photon polarization used here. To derive the Raman response, we proceed as usual [22] by relating the inelastic Raman scattering spectrum $I(\omega)$ to the dynamical susceptibility of the relevant mean field operator R: $I(\omega) = \frac{1}{2\pi}\int_{-\infty}^{\infty} dt\ e^{i\omega t}\langle R(t)R(0)\rangle$. The scattering spectrum I is related to the dynamical susceptibility χ'' by the fluctuation dissipation theorem: $I(\omega) = \chi''(\omega)/(1-e^{-\omega/T})$. Here, ω is the energy of the incident or scattered photon, and the operator R is the Loudon-Fleury photon-induced superexchange operator [28]

$$R = \sum_{\mathbf{r}_1,\mathbf{r}_2} (\hat{\mathbf{e}}_i \cdot \hat{\mathbf{r}}_{12})(\hat{\mathbf{e}}_s \cdot \hat{\mathbf{r}}_{12}) A(\mathbf{r}_{12}) \mathbf{S}_{r_1} \cdot \mathbf{S}_{r_2} \qquad (1)$$

For brevity, we will refer to R as a Raman operator. In (1), $\hat{\mathbf{r}}_{1,2}$ is the unit vector pointing from lattice site $\mathbf{r}_2$ to lattice site $\mathbf{r}_1$, and $\hat{\mathbf{e}}_i$ (respectively $\hat{\mathbf{e}}_s$) is the polarization vector of the incoming (outgoing) photon. The factor $A(\mathbf{r}_{12})$ is difficult to compute, but it is known that the ratio of A on different bonds is on the order of the spin-exchange couplings on the bonds (e.g. $A(\mathbf{r}_{j,j+2})/A(\mathbf{r}_{j,j+1})$ is $\mathcal{O}(J_2/J_1)$) [22]. Given a bare Hamiltonian H for a system, it is clear from the definition of $I(\omega)$ and (1) that two Raman operators R, R' yield the same spectrum if there exists some real constant C such that $R' = R - CH$. If such a C exists, we will say that R and R' are *spectrally equivalent*. Having reviewed some preliminary results on inelastic Raman scattering, we may consider the particular case of an isolated 1D magnetic chain.

Using the coordinate system of Fig. 1, a transverse *bb* polarization corresponds to $\theta_i = \theta_s = -\pi/2$. In this case the Raman operator is $R = R_1 \propto \sin^2\theta_0 \sum_j \mathbf{S}_j \cdot \mathbf{S}_{j+1}$. For a spin-1/2 nearest neighbor Heisenberg Hamiltonian, however, R_1 produces no spectrum (since it is proportional to the Hamiltonian) for this choice of polarization. By considering a next nearest neighbor interaction (2), the Raman operator is spectrally equivalent to R_1 and $R = R_2 \propto \sum_j \mathbf{S}_j \cdot \mathbf{S}_{j+2}$ for the *bb* polarization. In the limit of a straight chain ($\theta_0 \to 0$), the Raman operator vanishes (up to spectral equivalence), and no spinons are seen in the spectrum. Hence, both second neighbor interactions and a zig-zagged chain are sufficient conditions to observe spinons in the scattering spectrum for photon polarizations transverse (*bb*) to the chain axis.

We thus model the spinons with an antiferromagnetic J_1-J_2 Hamiltonian:

$$H_0 = \sum_j J_1 \mathbf{S}_j \cdot \mathbf{S}_{j+1} + J_2 \mathbf{S}_j \cdot \mathbf{S}_{j+2} \qquad (2)$$

with $J_1, J_2 > 0$. The quasi-1D chains of $Ba_3Ir_4O_{10}$ zigzag with a relative angle θ_0 as in Fig. 1a.

IV. RESULT OF THEORETICAL COMPUTATION

Within the minimal J_1-J_2 model (2), we compute the inelastic Raman scattering spectrum using a mean field theory of free 1D fermionic spinons [18]. We compute this spectrum using two equivalent choices of mean field (amounting to a choice between $R = R_1$ or R_2). The free spinon Hamiltonian is given by $H_0 = \sum_k \epsilon_k \hat{c}_k^\dagger \hat{c}_k$, where $\epsilon_k = -t\cos k = -\frac{\pi}{2} J_{\text{eff}} \cos k$. Here, we introduce an energy scale J_{eff}, which is a function of Hamiltonian parameters (J_1, J_2) scaled so that, in the $J_2 \to 0$ limit, it reproduces the exact Bethe ansatz result of $\epsilon_k = -\frac{\pi}{2} J_1 \cos(k)$ [29]. Wavevectors k are in units of inverse bond length projected onto the chain axis. The resulting inelastic scattering spectrum is then given by (3)

$$I^{(\nu)}(\omega) \propto \int_{-\pi}^{\pi} dk \int_{-\pi}^{\pi} dq \sum_{k'} \frac{h^{(\nu)}(k,k',q)[h^{(\nu)}(k,k',q) - h^{(\nu)}(k,k',k'-k-q)]}{\sqrt{(2t\sin(q/2))^2 + (\epsilon_{k+q} - \epsilon_k - \omega)^2}} \times f(\epsilon_k)(1-f(\epsilon_{k+q}))f(\epsilon_{k'})(1-f(\epsilon_{k'-q})) \tag{3}$$

where f is the Fermi function, $h^{(1)}(k,k',q) = \cos(q)$ and $h^{(2)}(k,k',q) = \cos(2q) - \cos(2k+q) - \cos(2k'-q)$, and the sum over k' is taken for all $k' \in [-\pi, \pi]$ which satisfy $2t\sin(q/2)\sin(k'-q/2) = \epsilon_{k+q} - \epsilon_k - \omega$.

The associated mean field four-spinon Raman susceptibility $\chi''_{R_\nu,R_\nu}(\omega)$ is plotted in Fig. 3 for $\nu = 1, 2$ at various temperatures. Here, χ''_{R_ν,R_ν} is the imaginary part of the dynamical susceptibility of R_ν. The low temperature hump feature agrees with experiment (Fig. 1b); at higher temperatures ($k_BT/J_{\rm eff} > 1$) the central frequency of the feature is lower, and the susceptibilities obtained from R_1 and R_2 become different. This difference quantifies the self-consistency breakdown of the theory at high temperatures.

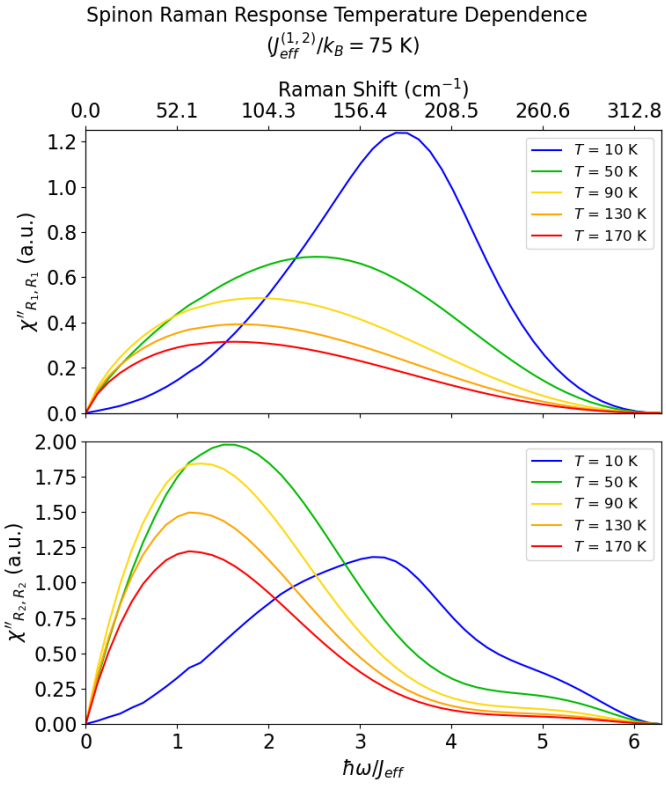

FIG. 3. Spinon Raman response computed within two mean field choices $R_{\nu=1,2}$, with $J_{\rm eff}^{(\nu)}/k_B = 75$ K at $T = 10, 50, 90, 130$ and 170 K (same vertical scale). The difference between R_1 and R_2 at higher temperatures quantifies the self-consistency breakdown of the Raman mean field theory.

The agreement between the mean field susceptibility and experiment at low temperature allows one to extract $J_{\rm eff}/k_B = 75$ K. The J_1-J_2 mean field self-consistency equation derived in Ref. [18] relates $J_{\rm eff}$ to a difference between J_1, J_2 in H_0: $J_{\rm eff} \approx 1.042J_1 - 0.8106J_2$, and the minus sign in this expression (arising from the sublattice-rotated Jordan-Wigner transformation into spinons) allows for a given $J_{\rm eff}$ to arise from substantially larger J_1, J_2. For example, taking $J_{\rm eff}/k_B = 75$ K as a reasonable energy scale for $Ba_4Ir_3O_{10}$, mean field self consistency permits $J_1/k_B = J_2/k_B = 324$ K. This scale for J_1, J_2 is consistent with Curie-Weiss measurements. For alpha$_c$ =J$_2$/J_1 ¡ 0.241, our result permits J_1 ¡ 88.6 K. This is closer to the lower end of the Curie-Weiss measurements (100-700 K), but arguably reasonable.

At higher temperatures the spinons are incoherent but nevertheless remain as the magnetic excitations. This is consistent with the broad damping feature persisting as temperature increases (Fig. 2). Now consider the sister magnetic material with Sr replacement. Where this magnet exhibits magnetic order, no broad peak is observed, but above T_N a broad peak similar to the pure case at high temperature appears. This interpretation suggests an intriguing possibility for the sister sample: the presence of the peak above T_N suggests that its magnetic transition could be considered as an instability of an incoherent parent quantum liquid state, "existing" (incoherently) at the high temperatures above T_N; strictly speaking this high temperature state is just a paramagnet, but here it evidently shows an unusually dense spectrum of strong short-ranged spin fluctuations, which could be interpreted as high-temperature relics of spinons.

As to using Raman to characterize the observed spinons, the model's agreement suggests they could be consistently modeled as 1D spinons within a low temperature effective theory, though we expect the spinons of any type of 2D quantum spin liquid phase to produce a similar four-spinon continuum hump. One intriguing possibility for a 2D quantum liquid phase with spinons closer to our model is the 2D "Bose-Luttinger Liquid" phase, a 2D bosonic generalization of 1D Luttinger Liquids recently introduced in Ref. [7]; its relevance would be resolved by observing appropriate singularities away from the Brillouin zone center.

V. PHONON LINEWIDTH BROADENING THROUGH SPIN-PHONON COUPLING

Due to the large unit cell and many allowed Raman modes, assignment of all observed phonon peaks to specific zone center vibrations requires detailed calculations and isotope substitution, which is outside the scope of this study. Still the origin of some of these peaks can be

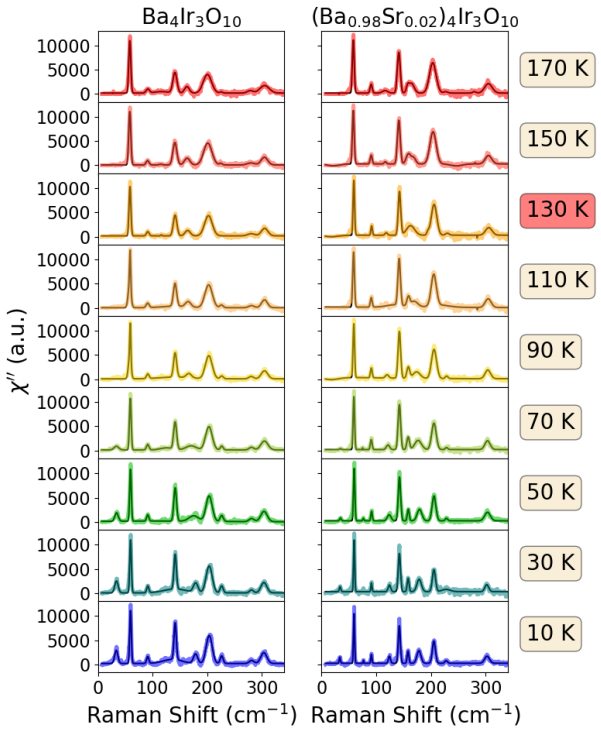

FIG. 4. Raman spectra in Fig. 2 with nonphononic contributions (background+electronic) subtracted. Dark solid lines show results of fitting of all phonon peaks to gaussians.

inferred based on correlating the phonon energies with particular features of the crystal structure. Ba is heavy and most loosely bonded atom, so we assign the peak at the low energy of 50 cm^{-1} to the Ba vibration. This peak is sharp in both samples (Fig. 1). Energies of the peaks between 100 and 250 cm^{-1} suggest that these phonons are associated with vibrations of the atoms belonging to the IrO_6 octahedra. They are expected to couple to magnetic excitations, and, therefore, show sensitivity to magnetic order and the quantum liquid behavior. Phonon broadening due to pseudospins that show short range correlation without long range magnetic order, combined with spin-orbit interaction [30], is well known e.g. in Sr_2IrO_4 at higher temperatures [31]. A similar effect is seen in our Sr-substituted $(Ba_{0.98}Sr_{0.02})_4Ir_3O_{10}$: Phonons gradually broaden and soften as the temperature is raised towards and above T_N.

Quantitative analysis of phonon lineshapes (width, intensity, and energy) as a function of temperature is complicated by the presence of the spinon continuum underneath the phonons as well as many overlapping peaks. In order to perform this analysis we first subtracted the background and the broad hump from the data, which isolated scattering intensity from the phonons only. Then the phonon intensities were fit to Gaussian lineshapes (Fig. 4). Lorentzian lineshapes give similar results for linewidths and peak positions, but fit quality is somewhat inferior. Because of some peak overlaps at some temperatures, we were able to obtain unambiguous results at all temperatures only for two peaks – at 140 cm^{-1} and 200 cm^{-1} as shown in Fig. 5.

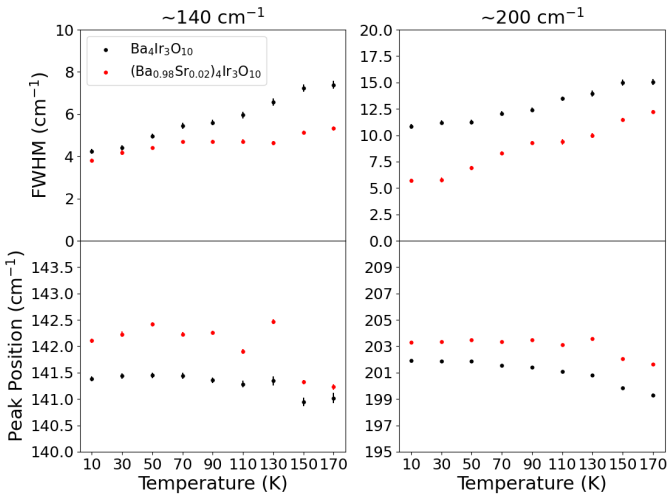

FIG. 5. Energies and linewidths of the phonon near 140 cm^{-1} and of the phonon near 200 cm^{-1}

Two types of behavior of phonon linewidths in our samples are illustrated in Fig. 5. The phonon at 140 cm^{-1} is typical of the first type where the linewidths of the phonons are similar in the doped and undoped samples at low temperatures, but the linewidth in the undoped sample increases faster as the temperature is raised. Qualitatively, the phonon at 175 cm^{-1} behaves similarly, with the caveat that its linewidth could not be reliably extracted at all temperatures due to its overlap with nearby modes. The phonon at 200 cm^{-1} (Fig. 5) characterises the second type. The peak is a factor of 2 narrower in the doped sample at low temperature with the difference between the two samples becoming smaller as the temperature is raised (about 20% at 170 K). The phonons at 90 and 160 cm^{-1} (Fig. 4) behave similarly at least qualitatively. The other phonons do not show strong temperature or doping dependence.

Most interestingly, broad phonons persist down to the lowest temperatures in pure $Ba_4Ir_3O_{10}$ (Fig. 2). The strongest effects occur in the phonons between 100 and 250 cm^{-1}. At low temperatures many phonons in the undoped sample are a factor of 2-3 broader than in the doped sample. This difference is far less dramatic at elevated temperatures where both samples are not magnetically ordered. This result is very striking because increased disorder presumably introduced by Sr substitution is expected to make the phonons broader, not narrower. In our interpretation, the electronic damping of the phonons due to magnetic fluctuations associated with the quantum liquid should not change much with tem-

perature in the undoped sample. The small broadening on heating is presumably due to reduced anharmonicity, which is not uncommon in oxides. This relatively small relative broadening with increasing temperature contrasts with a much stronger broadening (by as much as a factor of 4) in the doped sample where the effect is caused by a combination of increased magnetic fluctuations and anharmonicity. The low temperature narrowing of the phonon peaks upon Sr substitution, and indeed the broadened lineshapes in pure $Ba_4Ir_3O_{10}$ down to the lowest temperature, provide additional evidence for a quantum liquid with spinon excitations in $Ba_4Ir_3O_{10}$.

Fig. 5 shows that bigger linewidths are associated with lower phonon energies in agreement with standard self-energy effects. Beyond the particular quantum liquid state here, this behavior shows that strong coupling between magnetic degrees of freedom and phonons when the spin-orbit interaction is strong, exists at the lowest temperatures, not just near and above T_N as previously observed in Sr_2IrO_4. Interestingly here the broadened phonon peaks are symmetric and do not show any significant Fano lineshape. Thus the broad hump does not have a measurable interaction with phonons; instead, it appears that phonons are broadened by magnetic fluctuations that are not Raman active. This behavior dramatically illustrates that fluctuating disorder of the pseudospins in the quantum liquid phase dominates phonon damping at low temperatures for a large subset of phonons.

VI. THERMAL CONDUCTIVITY AND FUTURE OUTLOOK FOR THERMOELECTRICITY

The preceding discussion on phonon linewidth broadening by spinon-phonon scattering suggests that the suppressed phonon lifetimes should also be reflected in a reduced phonon contribution to thermal conductivity. Indeed the thermal conductivity shows this type of behavior with a surprisingly small value and an increase, within a window of low temperatures, upon Sr substitution [16]. That this observed thermal conductivity behavior can be mostly ascribed to phonon lifetimes is shown by the weak dependence of the thermal conductivity on applied magnetic fields within the quantum spin liquid state.

Such a quantum liquid with distinct phonon damping also presents a new direction for studies of thermoelectrics, in which poor phonon thermal conductivity is essential. Attempts to control thermal conductivity are focused on engineering structures that produce flat phonon bands [32]. Alternatively, phonon lifetime can be reduced via damping by interactions with other phonons, defects, or electrons [33]. But this type of phonon damping necessarily accompanies an unwanted consequence of reduced electrical conductivity. It is also established that spin-phonon coupling via magnetostriction can reduce the phonon lifetime, thus suppress phonon thermal conductivity [34]. Here we demonstrate that spin-orbit interaction, rather than magnetostriction, can be an efficient driver of phonon damping, which extends possible thermoelectricity to a new class of materials: magnetically non-ordered 4d and 5d transition metal materials with strong spin-orbit interaction. When these exhibit strongly correlated conducting phases, rather than Mott insulators, the spin sector of the conducting electrons may still damp phonons in analogy to the spinon-phonon coupling mechanism in the present Mott insulator case.

We thank Martin Mourigal, Zhigang Jiang, and Michael Pustilnik for helpful conversations. I.K. acknowledges the Aspen Center for Physics where part of this work was performed, which is supported by National Science Foundation grant PHY-1607611. Work at the University of Colorado was funded by the U.S. Department of Energy, Office of Basic Energy Sciences, Office of Science, under Contract No. DE-SC0006939 and by National Science Foundation grant DMR-1903888.

[1] X. G. Wen, Mean-field theory of spin-liquid states with finite energy gap and topological orders, Phys. Rev. B **44**, 2664 (1991).
[2] A. Kitaev, Anyons in an exactly solved model and beyond, Annals of Physics **321**, 2 (2006).
[3] L. Savary and L. Balents, Quantum spin liquids: a review, IOP Publishing **80**, 016502 (2016).
[4] Y. Zhou, K. Kanoda, and T.-K. Ng, Quantum spin liquid states, Rev. Mod. Phys. **89**, 025003 (2017).
[5] L. Balents, Spin liquids in frustrated magnets, Nature **464**, 199 (2010).
[6] R. Mukhopadhyay, C. L. Kane, and T. C. Lubensky, Sliding luttinger liquid phases, Phys. Rev. B **64**, 045120 (2001).
[7] E. Lake, T. Senthil, and A. Vishwanath, Bose-luttinger liquids, Phys. Rev. B **104**, 014517 (2021).
[8] J. c. v. Chaloupka, G. Jackeli, and G. Khaliullin, Kitaev-heisenberg model on a honeycomb lattice: Possible exotic phases in iridium oxides A_2IrO_3, Phys. Rev. Lett. **105**, 027204 (2010).
[9] G. Jackeli and G. Khaliullin, Mott insulators in the strong spin-orbit coupling limit: From Heisenberg to a quantum compass and Kitaev models, Phys. Rev. Lett. **102**, 017205 (2009).
[10] W. Witczak-Krempa, G. Chen, Y. B. Kim, and L. Balents, Correlated quantum phenomena in the strong spin-orbit regime, Annual Review of Condensed Matter Physics **5**, 57 (2014).
[11] J. G. Rau, E. K.-H. Lee, and H.-Y. Kee, Spin-orbit physics giving rise to novel phases in correlated systems: Iridates and related materials, Annual Review of Condensed Matter Physics **7**, 195 (2016).
[12] G. Cao and P. Schlottmann, The challenge of spin–orbit-tuned ground states in iridates: a key issues review, Reports on Progress in Physics **81**, 042502 (2018).
[13] M. Hermanns, I. Kimchi, and J. Knolle, Physics of the Kitaev model: Fractionalization, dynamic correlations,

and material connections, Annual Review of Condensed Matter Physics **9**, 17 (2018).
[14] J. Nasu, J. Knolle, D. L. Kovrizhin, Y. Motome, and R. Moessner, Fermionic response from fractionalization in an insulating two-dimensional magnet, Nature Physics **12**, 912 (2016).
[15] H. Takagi, T. Takayama, G. Jackeli, G. Khaliullin, and S. E. Nagler, Concept and realization of Kitaev quantum spin liquids, Nat. Rev. Phys. **1**, 264 (2019).
[16] G. Cao, H. Zheng, H. Zhao, Y. Ni, C. A. Pocs, Y. Zhang, F. Ye, C. Hoffmann, X. Wang, M. Lee, *et al.*, Quantum liquid from strange frustration in the trimer magnet $Ba_4Ir_3O_{10}$, npj Quantum Materials **5**, 1 (2020).
[17] M. Udagawa, H. Aoki, N. Ogita, O. Fujita, A. Sohma, A. Ogihara, and J. Akimitsu, Raman scattering of $CuGeO_3$, Journal of the Physical Society of Japan **63**, 4060 (1994).
[18] W. Brenig, Raman scattering from frustrated quantum spin chains, Phys. Rev. B **56**, 2551 (1997).
[19] M. Hase, I. Terasaki, and K. Uchinokura, Observation of the spin-Peierls transition in linear Cu^{2+} (spin-1/2) chains in an inorganic compound $CuGeO_3$, Phys. Rev. Lett. **70**, 3651 (1993).
[20] P. Van Loosdrecht, J. Boucher, G. Martinez, G. Dhalenne, and A. Revcolevschi, Inelastic light scattering from magnetic fluctuations in $CuGeO_3$, Phys. Rev. lett. **76**, 311 (1996).
[21] M. Braden, B. Hennion, W. Reichardt, G. Dhalenne, and A. Revcolevschi, Spin-phonon coupling in $CuGeO_3$, Phys. Rev. Lett. **80**, 3634 (1998).
[22] M. Sato, H. Katsura, and N. Nagaosa, Theory of Raman scattering in one-dimensional quantum spin-1/2 antiferromagnets, Phys. Rev. Lett. **108**, 237401 (2012).
[23] V. Kiryukhin and B. Keimer, Incommensurate lattice modulation in the spin-Peierls system $CuGeO_3$, Phys. Rev. B **52**, R704 (1995).
[24] G. Sala, M. B. Stone, B. K. Rai, A. F. May, P. Laurell, V. O. Garlea, N. P. Butch, M. D. Lumsden, G. Ehlers, G. Pokharel, A. Podlesnyak, D. Mandrus, D. S. Parker, S. Okamoto, G. B. Halász, and A. D. Christianson, Van hove singularity in the magnon spectrum of the antiferromagnetic quantum honeycomb lattice, Nature Communications **12**, 171 (2021).
[25] R. R. P. Singh, P. Prelovšek, and B. S. Shastry, Magnetic Raman scattering from 1D antiferromagnets, Phys. Rev. Lett. **77**, 4086 (1996).
[26] V. Muthukumar, C. Gros, W. Wenzel, R. Valentí, P. Lemmens, B. Eisener, G. Güntherodt, M. Weiden, C. Geibel, and F. Steglich, Frustration-induced raman scattering in $CuGeO_3$, Phys. Rev. B **54**, R9635 (1996).
[27] G. Gómez-Santos, Role of domain walls in the ground-state properties of the spin-1/2 *XXZ* Hamiltonian in the linear chain, Phys. Rev. B **41**, 6788 (1990).
[28] P. A. Fleury and R. Loudon, Scattering of light by one- and two-magnon excitations, Phys. Rev. **166**, 514 (1968).
[29] J. des Cloizeaux and J. J. Pearson, Spin-wave spectrum of the antiferromagnetic linear chain, Phys. Rev. **128**, 2131 (1962).
[30] H. Liu and G. Khaliullin, Pseudo-Jahn-Teller effect and magnetoelastic coupling in spin-orbit Mott insulators, Phys. Rev. Lett. **122**, 057203 (2019).
[31] H. Gretarsson, N. Sung, M. Höppner, B. Kim, B. Keimer, and M. Le Tacon, Two-magnon Raman scattering and pseudospin-lattice interactions in Sr_2IrO_4 and $Sr_3Ir_2O_7$, Phys. Rev. Lett. **116**, 136401 (2016).
[32] M. Christensen, A. B. Abrahamsen, N. B. Christensen, F. Juranyi, N. H. Andersen, K. Lefmann, J. Andreasson, C. R. Bahl, and B. B. Iversen, Avoided crossing of rattler modes in thermoelectric materials, Nature Materials **7**, 811 (2008).
[33] M. Ikeda, H. Euchner, X. Yan, P. Tome¥vs, A. Prokofiev, L. Prochaska, G. Lientschnig, R. Svagera, S. Hartmann, E. Gati, *et al.*, Kondo-like phonon scattering in thermoelectric clathrates, Nature Communications **10**, 1 (2019).
[34] D. Bansal, J. L. Niedziela, A. F. May, A. Said, G. Ehlers, D. L. Abernathy, A. Huq, M. Kirkham, H. Zhou, and O. Delaire, Lattice dynamics and thermal transport in multiferroic $CuCrO_2$, Phys. Rev. B **95**, 054306 (2017).